

Upregulated miR-486 Induces Therapeutic Angiogenesis and Improves Infarction Recovery in Rat Myocardial Ischemia Model

Hong-Wei Qi

Cardiovascular Center, Beijing Tongren Hospital, Capital Medical University

Hai-Tao Zhang

Chengde Medical University Affiliated Hospital

Hui-Yan Sun

Yanda Medical Research Institute

Lin Zhang

Affiliated Hospital of Medical College Qingdao University: The Affiliated Hospital of Qingdao University

Yang Sun

Affiliated Hospital of Medical College Qingdao University: The Affiliated Hospital of Qingdao University

Li-Sheng Wang

Affiliated Hospital of Medical College Qingdao University: The Affiliated Hospital of Qingdao University

Biao Yuan (✉ yuan.biao@live.cn)

Beijing Tongren Hospital <https://orcid.org/0000-0001-5098-8078>

Research article

Keywords: Rat acute myocardial model, MicroRNA-486, Adenovirus, Gene therapy

Posted Date: February 4th, 2021

DOI: <https://doi.org/10.21203/rs.3.rs-171054/v1>

License:   This work is licensed under a Creative Commons Attribution 4.0 International License.

[Read Full License](#)

Abstract

Background

Besides hematopoietic cells, miR-486 is also enriched in cardiac, skeletal, and smooth muscles. However, its roles in regulating the function of cardiomyocytes and tissue repair in myocardial infarction have not been explored yet.

Methods

We investigated the effects of miR-486 on the survival and hypoxic response of cardiomyocytes. Also, using adenovirus-mediated overexpression, we evaluated its therapeutic effects in myocardial repair in a rat acute myocardial infarct (AMI) model.

Results

Hypoxia treatment upregulated miR-486 in cardiomyocytes. Moreover, adenovirus-mediated overexpression of miR-486 reduced cell injury, increased cell viability, and decreased apoptosis in hypoxic conditions. In a rat AMI model, administration of Ad-miR-486 reduced infarct size and collagen deposition, increased vessel density, and improved cardiac function. Furthermore, *in vivo* data suggest that the protective effects of miR-486 in cardiomyocytes were related to its anti-apoptotic function.

Conclusion

miR-486 overexpression protects myocytes from hypoxia-induced apoptosis and has therapeutic potential in myocardial infarction.

Highlights

1. Hypoxia upregulates miR-486 in cardiomyocytes
2. miR-486 overexpression improves heart function in rat AMI model
3. miR-486 induces angiogenesis and enhance the survival of cardiomyocytes

Introduction

Acute myocardial infarction (AMI) is one of the critical cardiovascular diseases. Although many novel regenerative approaches such as stem cell transplantation and angiogenic gene therapy have received significant attention^[1-3], these have limited clinical effectiveness due to lower engraftment efficacy and impaired angiogenic ability^[4, 5]. Thus, it is essential to extensively elucidate the pathogenesis of AMI to develop novel approaches for the repair of infarct myocardium.

MicroRNAs (miRNAs), a kind of small non-coding regulatory RNAs, are associated with various diseases. Accumulating evidence suggests that miRNAs might play critical roles in ischemia heart disease^[6, 7]

regulating fundamental components of the disease pathogenesis and progression^[8, 9]. A multitude of miRNAs have been linked to vascular development, homeostasis, function, disease, and regeneration^[10]. In addition to hematopoietic cells, miR-486, a multi-functional miRNA, is enriched in cardiac, skeletal, and smooth muscles. It was first found in the human fetal liver cDNA library and has been located in the last intron of the Ankyrin-1 (Ank1) gene^[11]. Several reports showed that miR-486 is an erythroid related miRNA that plays important regulatory roles in hematopoiesis and leukemogenesis^[12-14]. Notably, miR-486 is also considered as a tumor suppressor and often down-regulated in non-small cell lung cancer (NSCLC) and hepatoma^[15]. In several tumors including lung cancer, the expression of miR-486 is regulated by the methylation of its host gene Ank1^[16].

Interestingly, a recent study showed that miR-486 is a hypoxia response miRNA and regulates the angiogenic activity of bone marrow-derived mesenchymal stem cells^[17]. In myocytes, miR-486 is transcriptionally controlled by SRF and MRTF-A, as well as by MyoD, and regulates the phosphatase and tensin homolog (PTEN) and FOXO1a (FOXO1, Forkhead Box O1) to negatively affect the phosphoinositide-3-kinase (PI3K)/AKT signaling^[18]. A rat study showed that miR-486 protects cardiomyocytes from apoptosis through targeting PTEN and activating the PI3K/AKT pathway^[19]. However, its role in regulating cardiomyocyte function and AMI pathogenesis has not been explored yet. Given the importance of miR-486 in angiogenesis and hypoxia, we hypothesize that it might also modulate the functions of myocytes and affect AMI pathogenesis. In this study, we investigated the effects of miR-486 overexpression in cardiomyocytes to reveal its potential therapeutic effects in AMI.

Materials And Methods

Experimental animals

The Sprague-Dawley (SD) rats were obtained from the Animal Center of Academy of Military Medical Sciences, Beijing, China. A total of 120 healthy adult SD rats (age, 6–8 weeks; 200±20 g; both males and females) and 15 healthy neonatal rats (aged 24–48 h; 6.3±1.4 g; both males and females) were maintained under controlled conditions (20–25°C; relative humidity 40–60%; 12 h light/dark cycle with food and water *ad libitum*). Animals were handled as per the guidelines of the Institutional Animal Care and Use Committee of Capital Medical University. All experiments were performed following the National Institutes of Health guide for the care and use of laboratory animals and the guidelines of the International Association for the Study of Pain. The rats were anesthetized with isoflurane (adult SD rats with 1.87%; neonatal rats with 1.6%) and euthanized by cervical dislocation.

Isolation and culture of cardiomyocytes

Primary cultures of neonatal rat cardiac ventricular myocytes were performed as described previously^[20, 21]. Briefly, the hearts from 1-2 day(s) old SD rats were removed after hypothermia anesthesia by immersion in ice water and placed in ice-cold 1× phosphate-buffered saline solution. After repeated rinsing, the atria were cut off, and the ventricles were minced with scissors. The minced tissue and

ventricular cells were dispersed by digestion with collagenase type IV (0.45 mg/ml), 0.1% trypsin, and 15 µg/ml DNase I. Cardiomyocytes were cultured in the cardiac myocyte culture medium containing Dulbecco's modified Eagle's medium supplemented with 10% serum, 4 µg/ml transferrin, 0.7 ng/ml sodium selenite, 2 g/L bovine serum albumin (fraction V), 3 mmol/L pyruvic acid, 15 mmol/L HEPES, 100 µmol/L ascorbic acid, 100 µg/ml ampicillin, 5 µg/ml linoleic acid, 1% penicillin and 1% streptomycin, and 100 µmol/L 5-bromo-2'deoxyuridine. The cells were seeded into six-well plates. The myocytes were passaged and used for *in vitro* studies.

Adenoviral vectors and cardiomyocyte gene transfection

The adenovirus vector carrying rat miR-486 gene was generated from Adeno-XTM Expression Systems (Clontech) according to the manufacturer's protocols. The replication-defective recombinant adenovirus was amplified in HEK293 cells and purified by cesium chloride gradient ultracentrifugation. The final plaque-forming units (pfu) were estimated by titration in HEK293 cells using agarose overlay. The cardiomyocytes were infected with the recombinant adenovirus at MOI (multiplicity of infection) of 150. The infection efficiency was determined based on the percentage of GFP+ cells in transduced cardiomyocytes.

For miR-486 inhibitor transfection, cardiac myocytes were cultured and transfected with siRNA by nucleofection. The transduced cardiac myocytes were transferred to the completed medium, cultured for 24 h, and then subjected to proliferation and apoptosis assays.

RNA Extraction and TaqMan miRNA assay

Total RNA was extracted from tissues/cells using the Trizol Reagent and cDNA synthesis was performed with the Taqman@ MicroRNA Reverse Transcription Kit (Thermo, USA). miR-486 and U6 (internal control) were amplified according to the TaqMan MicroRNA assay protocol (Applied Biosystems, USA). The assays were carried out in triplicates and the relative quantitative evaluation of the target gene levels was performed by comparing $\Delta\Delta Ct$.

The rat AMI model and treatment

A schematic of our experimental approach is shown in Fig. 1. Experimental AMI was induced as described previously. Briefly, to establish the rat AMI model, adult SD rats were anesthetized and surgery was performed to ligate the left anterior descending coronary artery. The rats (number 120, weight 200 ± 20 g) were divided into four groups, namely the sham group, AMI group, adenovirus group (Ad-ctr), and Ad-miR-486 group. In the last two groups, the AMI rats were treated with control virus and Ad-miR-486 respectively. The adenovirus was injected into the border zone surrounding the infarcts using a 27G needle.

Measurement of left ventricles ejection fraction (LVEF) and left ventricular fractional shortening (LVFS)

Four weeks after establishing AMI in rats, echocardiographic examinations were performed after intraperitoneal injection with Chloral hydrate (10%, 3ml/100g) and using the Vevo770 ultrasound system (Visualsonics Inc., Toronto, Canada). The electrode of the Vevo770 ultrasound system was attached to the animal using adhesive plaster and the ECG was monitored. The hairs on the rat chest were removed with depilatory creams. Left ventricular end-diastolic diameters (LVEDD) and left ventricular end-systolic diameters (LVESD) were measured using the ultrasound coupler (Fig. 2). Based on the measurements, LVEF and LVFS were calculated. At least three successive records were used to calculate the average value.

Infarct size, collagen deposition, and vessel density

The rats were sacrificed at 4 weeks after AMI. After hemodynamic studies, the animals were sacrificed to remove hearts. These were perfused with PBS for rinsing and frozen quickly. Myocardial infarct size was determined by pathological staining, a gold standard in AMI studies. The heart ventricles were sliced transversely into 2 mm thick slices and incubated in 1% triphenyltetrazolium chloride (TTC) at 37°C for 15 min to identify the noninfarcted and infarcted areas. TTC staining displayed a red color. TTC unstained area (white color) defined the infarcted area and the size was expressed as a percentage of the ischemic area.

Microvessel density was evaluated based on CD-31 expression and calculated. The microvessel endothelial cell membranes were highlighted by staining using the anti-CD-31 antibodies. Any cluster of endothelial cells that was markedly separated from the adjacent microvessel was considered a vessel. Then, five random nonoverlapping 400x high-power fields around the MI area were selected and on average, 5 such records were counted on each slide.

Measurement of collagen volume fraction (CVF) by Masson's trichrome staining

Rats were sacrificed at 4 weeks after AMI. Hearts were excised and soaked immediately in saline to remove the excess blood from the ventricles. These were fixed in 4% triformol. Paraffin-embedded samples were sectioned at 5 µm to perform the Masson's trichrome staining. Digital images of the stained sections were captured and CVF was analyzed using the Image Pro-Plus 6.0 software. CVF is expressed as a percentage of the collagen area in the whole field and calculated as the average of 5 random AMI fields in each slide.

Measurement of myocardium apoptotic index (AI)

Rats were sacrificed at 4 weeks after AMI. The tissue sections from the heart were stained with TUNEL. Five consecutive nonoverlapping 400x high-power fields were selected and the average counts of total and apoptotic cells were calculated. The AI was determined using the formula: the number of apoptotic cells/total cells × 100%.

Cell proliferation and apoptosis assays

The proliferation of cardiac myocytes was determined with CCK-8 assay. Cell apoptosis was determined by AnnexinV-APC staining. Briefly, the cardiac myocytes were cultured in a completed culture medium at 37°C for 48 h. The cells were treated with trypsin, washed with cold PBS, and resuspended in Annexin-V binding buffer. Then, the cells were stained with Annexin V-APC to detect apoptotic cells by flow cytometry.

Statistics

All data are presented as mean \pm S.E. p-value < 0.05 was considered statistically significant.

Results

Hypoxia upregulated miR-486 in cardiomyocytes

Cardiomyocytes were isolated from neonatal SD rats and cultured for expansion in 1% O₂ for different periods. Then, the expression of miR-486 was estimated using qRT-PCR. We observed that in a hypoxic environment, the cardiomyocytes exhibited upregulation of miR-486 at 6 h which reached to maximum at 24 h (Fig. 3A). This suggests that miR-486 is a hypoxia response miRNA in cardiomyocytes.

Upregulation of miR-486 protected cardiomyocytes from hypoxia-induced apoptosis

Next, we evaluated the regulatory effect of miR-486 on cardiomyocytes. For this, the cardiomyocytes were transfected with miR-486 inhibitors or mimics and cultured in hypoxia for 6 h to estimate the cell viability, LDH activity, and apoptosis. We observed that miR-486 inhibitor transfected cardiomyocytes exhibited a significant increase in hypoxia-induced apoptosis and LDH release while the cell viability was decreased. Whereas transfection with miR-486 led to decreased apoptosis and LDH release while increasing the cell viability, compared to the control group (Fig. 3B-D). It indicates that miR-486 expression protected the cardiomyocytes from hypoxia-induced apoptosis.

Adenovirus-mediated expression of miR-486 improved heart function in the rat AMI model

The mortality rate in the Sham group was 6.67%. Unfortunately, the rat mortality rate after AMI increased to 20%. However, the differences were not significant enough ($P \geq 0.05$).

To elucidate the role of miR-486 upregulation in cardiomyocyte functions, *in vivo* study using the adenovirus-mediated miR-486 overexpression was performed in the rat AMI model. The Ad-miR-486 and Ad-GFP control vector were injected into the myocardium and the expression of miR-486 was determined by qRT-PCR in the tissue lysate obtained from the injected area. Treatment with Ad-miR-486 resulted in high levels of miR-486 in the myocardium. However, after one month of treatment, the adenovirus-mediated increase in miR-486 expression gradually returned to the basal level (Fig. 4A).

Then, four weeks post adenovirus administration, the heart functional parameters were determined in both Ad-miR-486 and control vector treated rat AMI models. We found that the treatment with Ad-miR-486

improved the cardiac function significantly. Fig. 4B shows the comparison of functional changes by echocardiography. We observed that compared to animals in the sham group, LVEF and LVFS were significantly lower in the MI and Ad-ctr group ($P \leq 0.05$). However, upon Ad-miR-486 treatment, LVEF and LVFS were significantly increased in the rat AMI model (Fig. 4C-D). It suggests that Ad-miR-486 therapy can benefit in AMI. Although, we did not observe any significant differences in the survival curves of the four groups ($P \leq 0.05$). (Fig. 5)

Ad-miR-486 transduction reduced infarction size and fibrosis in the rat AMI model

At 4 weeks after Ad-miR-486 therapy, compared to the control vector group, the heart infarcted size decreased and wall thickness increased in the Ad-miR-486 group. The heart infarcted size in the AMI group, Ad-ctr group, and Ad-miR-486 group were $35.81 \pm 1.51\%$, $35.05 \pm 1.75\%$, and $30.75 \pm 1.96\%$ respectively (Fig. 6A-B).

Moreover, four weeks after AMI, the infarcted areas were subjected to histological evaluations using the hematoxylin-eosin staining. The collagen content in the noninfarcted area was stained with collagen-specific Sirius red (Fig. 6C). We found that the collagen volume fraction was significantly lower in the Ad-miR-486 group compared to the Ad-ctr groups. Also, treatment with Ad-miR-486 markedly reduced the interstitial fibrosis in the non-infarcted myocardium. The pictures were analyzed using the Image-Pro Plus 6.0 image analysis system. The CVF in the AMI group, Ad-ctr group, and Ad-miR-486 group were significantly higher than the sham group ($P \leq 0.05$). The CVF in the Ad-miR-486 group was significantly lower than the AMI group and Ad-ctr group ($P \leq 0.05$). Notably, there was no significant difference between the AMI group and Ad-ctr group ($P \leq 0.05$) (Fig. 6D).

Ad-miR-486 treatment increased microvessel density (MVD) and the survival of cardiomyocytes in the rat AMI model

Meanwhile, we evaluated the vascular density in the infarcted areas. We found that compared to the sham group, AMI group, and Ad-ctr group, MVD was significantly higher ($P < 0.05$, $n = 6/\text{group}$) in the Ad-miR-486 group (Fig. 7A-B). Moreover, we did not observe any significant difference between the AMI and Ad-ctr groups ($P \leq 0.05$).

To examine the potential cellular mechanism of miR-486-mediated protection against myocardial infarction, we performed *in vivo* analysis of apoptosis in infarcted heart sections by immunofluorescence using TUNEL staining. The representative TUNEL-stained photomicrographs of heart sections from Ad-miR-486 treated rats are shown in Fig. 8A. Notably, we found that in the infarcted areas, the apoptosis of the cardiac cells significantly decreased in the Ad-miR-486-treated group (Fig. 8B). This indicates that the protective mechanism of miR-486 against myocardial infarction could be related to its anti-apoptotic effect in the cardiomyocytes.

Discussion

miRNA dysregulation has been linked to the initiation and pathogenesis of several diseases including cancer and cardiovascular ischemia^[22-24]. Particularly, in myocardial infarction, several miRNAs are gaining huge interest as putative novel disease biomarkers and therapeutic targets^[25]. miR-486, a hypoxia response miRNA, has multiple functions including angiogenic activities^[26]. Notably, it was found downregulated in the muscles of dystrophin-deficient mice and DMD (Duchenne muscular dystrophy) patients^[17]. Previous studies strongly suggest that miR-486 regulates the function of cardiomyocytes and plays a vital role in cardiovascular ischemia. In this study, we transduced rat cardiomyocytes with the miR-486 gene to investigate its protective effects in hypoxia-induced apoptosis. Furthermore, it was examined for potential therapeutic benefits in a rat AMI model.

Our *in vitro* studies revealed that in hypoxic conditions, the levels of miR-486 were highly upregulated in the cultured cardiomyocytes. Therefore, we next investigated the protective effects of miR-486 on the survival of cardiomyocytes. Interestingly, results from LDH release and apoptosis assay suggest that upregulated miR-486 or transduction with its mimics significantly increased the survival of cardiomyocytes in hypoxia. On contrary, transduction with miR-486 inhibitor suppressed the growth and survival of cardiomyocytes. Meanwhile, multiple apoptosis and angiogenesis-related genes, such as PTEN, FOXO1, and Sirt1, identified as the targets of miR-486, were examined for their role in cardiomyocytes resistance against hypoxia-induced apoptosis. Notably, PTEN is a known negative regulator of H₂O₂-induced apoptosis in rat cardiomyocytes^[27]. Interestingly, a recent report revealed that exosomal miR-486-5p carrying mesenchymal stromal cells suppresses cardiomyocyte apoptosis under ischemic and hypoxic conditions via targeting the PTEN/PI3K/AKT signaling pathway. It seems that miR-486 overexpression suppresses the PTEN molecules, leading to activation of the PI3K/AKT pathway, which enhances the cardiomyocyte survival. Importantly, it has also been reported that miR-486-5p targeting PTEN protects against coronary microembolization-induced apoptosis in rat cardiomyocytes by activating the PI3K/AKT pathway. FOXO1 regulates myocardial glucose oxidation via transcriptional control of pyruvate dehydrogenase kinase 4^[28]. Also, its inhibition significantly suppresses the myoblast proliferation and induces myoblast apoptosis^[29]. Likewise, SIRT1 deactivation plays a key role in ischemia-reperfusion-induced apoptosis^[30]. Besides, miR-486-5p is known to repress MRTF-A affecting a complex network of transcriptional and post-transcriptional regulatory mechanisms in myogenesis. Therefore, one can speculate that miR-486 mediated regulation of aforesaid targets could potentially contribute to its protective effects in cardiomyocytes.

We found that Ad-miR-486 administration showed therapeutic benefits in a rat AMI model. Its overexpression improved the heart functions including a decrease in LVEDP, suggesting improvement in ventricular remodeling. Our results suggest that the potential mechanisms for the therapeutic effect of Ad-miR-486 in infarct myocardium include inhibition of apoptotic pathways and induced angiogenesis. Furthermore, our *in vitro* transfection studies verified that miR-486 expression improved the survival of myocardial myocytes. It was reported that exosomal miRNAs-486-5p mediates wound healing by promoting angiogenesis. Also, it is a familiar fact that therapeutic angiogenesis in stem cell/gene therapy largely depends on multiple angiogenic growth factors. For instance, miR-486 transduced bone marrow

stromal cells secrete increased levels of soluble angiogenic proteins such as VEGF and HGF, which induce therapeutic angiogenesis and has been shown to improve cardiac function in a rat AMI model^[17]. Treatment with Ad-miR-486 also inhibited fibrosis in infarcted myocardium in AMI models. This phenomenon is in agreement with a recent report that showed anti-fibrotic effects of miR-486 in the pulmonary fibrosis model^[31]. Notably, SMAD2, a crucial mediator of pulmonary fibrosis, is targeted by miR-486^[31]. In this study, both *in vitro* and *in vivo* investigations revealed that miR-486 overexpression protects cardiomyocytes from apoptosis and thereby improves infarction recovery.

Conclusion

Ad-miR-486 has the therapeutic effects in infarcted myocardium which involved increased angiogenesis, suppressed apoptosis, and reduction in myocardial fibrosis. Therefore, miR-486 gene therapy could be a potential therapeutic strategy in AMI.

Abbreviations

Ad-ctr: adenovirus group; AI: apoptotic index; AMI: acute myocardial infarct; Ank1: Ankyrin-1; CVF: collagen volume fraction; DMD: Duchenne muscular dystrophy; FOXO1: Forkhead Box O1; LVEDD: left ventricular end-diastolic diameters; LVEF: left ventricles ejection fraction; LVESD: left ventricular end-systolic diameters; LVFS: left ventricular fractional shortening; miRNAs: microRNAs; MOI: multiplicity of infection; MVD: microvessel density; NSCLC: non-small cell lung cancer; PI3K: phosphoinositide-3-kinase; PTEN: phosphatase and tensin homolog; SD: Sprague-Dawley; TTC: triphenyltetrazolium chloride

Declarations

Availability of data and materials

Datasets used or analysed during the current study are available from the corresponding author on reasonable request.

Contributions

Qi HW: conception/design, drafting manuscript, revision, final approval. Zhang HT: animal experiment, data collection. Sun HY: conception/design, experimental advice. Zhang L: cell experiment, data collection. Sun Y: cell experiment, data collection. Wang LS (corresponding author): conception/design, final approval. Yuan B (corresponding author): experimental advice, final approval.

Ethics approval

This study was approved by the Institutional Laboratory Animal Care and Use Committee of Capital Medical University (Beijing, China).

Consent for publication

Not applicable.

Funding

This study was supported by the Chinese National Science Foundation Committee Grant (No. 81370237).

Competing interests

The authors declare that they have no competing interests.

Acknowledgements

We thank Dr. Ying Bai (Cardiovascular Center, Beijing Tongren Hospital, Capital Medical University) for statistical advice.

References

1. Shafei, A.E.a., et al., *Mesenchymal stem cell therapy: A promising cell-based therapy for treatment of myocardial infarction*. Journal of Gene Medicine, 2017. **19**(12): p. e2995.
2. Wang, L., et al., *Hepatocyte Growth Factor Gene Therapy for Ischemic Diseases and Tissue Regeneration*. Human Gene Therapy, 2018: p. 413-423.
3. Anwaruddin, S., *Stem cell therapy for ischemic heart disease*. Trends in Molecular Medicine, 2003. **9**(10): p. 436-441.
4. Rubanyi and M. Gabor, *Identifying and overcoming obstacles in angiogenic gene therapy for myocardial ischemia*. Journal of Cardiovascular Pharmacology, 2014. **64**(2): p. 109-19.
5. Lima, J., et al., *MicroRNAs in Ischemic Heart Disease: From Pathophysiology to Potential Clinical Applications*. Cardiology in Review, 2016. **25**(3): p. 1.
6. Sala, V., et al., *MicroRNAs in myocardial ischemia: identifying new targets and tools for treating heart disease. New frontiers for miR-medicine*. Cellular & Molecular Life Sciences, 2014. **71**(8): p. 1439-1452.
7. Canfrán-Duque, A., et al., *Micro-RNAs and High-Density Lipoprotein Metabolism*. Arterioscler Thromb Vasc Biol, 2016: p. 1076.
8. Feinberg, M.W. and K.J. Moore, *MicroRNA Regulation of Atherosclerosis*. Circulation Research, 2016. **118**(4): p. 703.
9. Kane, N.M., et al., *Concise Review: MicroRNAs as Modulators of Stem Cells and Angiogenesis*. STEM CELLS, 2014. **32**(5).
10. Fu, H., et al., *Identification of human fetal liver miRNAs by a novel method*. Febs Letters, 2005. **579**(17): p. 3849-3854.
11. *MicroRNA-486-5p is an erythroid oncomiR of the myeloid leukemias of Down syndrome*. Blood, 2015. **125**(8): p. 1292-301.

12. Wang, L.S., et al., *MicroRNA-486 regulates normal erythropoiesis and enhances growth and modulates drug response in CML progenitors*. Blood, 2015. **125**(8): p. 1302.
13. Leighton, et al., *A 2-way miRror of red blood cells and leukemia*. Blood, 2015.
14. Tessema, M., et al., *ANK1 Methylation regulates expression of MicroRNA-486-5p and discriminates lung tumors by histology and smoking status*. Cancer Letters, 2017: p. 191.
15. Sun, H., et al., *miR-486 regulates metastasis and chemosensitivity in hepatocellular carcinoma by targeting CLDN10 and CITRON*. Hepatol Res, 2015. **45**(13): p. 1312-22.
16. Tessema, M., et al., *ANK1 Methylation regulates expression of MicroRNA-486-5p and discriminates lung tumors by histology and smoking status*. Cancer Lett, 2017. **410**: p. 191-200.
17. Shi, X.F., et al., *MiRNA-486 regulates angiogenic activity and survival of mesenchymal stem cells under hypoxia through modulating Akt signal*. Biochemical & Biophysical Research Communications, 2016: p. 670-677.
18. Shyu, K.G., et al., *Intramyocardial injection of naked DNA encoding HIF-1 α /VP16 hybrid to enhance angiogenesis in an acute myocardial infarction model in the rat*. Cardiovascular Research, 2002. **54**(3): p. 576.
19. Zhu, H.H., et al., *MicroRNA-486-5p targeting PTEN Protects Against Coronary Microembolization-Induced Cardiomyocyte Apoptosis in Rats by activating the PI3K/AKT pathway*. European Journal of Pharmacology, 2019. **855**: p. 244-251.
20. Sreejit, et al., *An improved protocol for primary culture of cardiomyocyte from neonatal mice*. Vitro Cellular & Developmental Biology Animal, 2008.
21. Tao, J., et al., *[An improved protocol for primary culture of cardiomyocyte from neonatal rat.]*. Zhonghua xin xue guan bing za zhi Chinese journal of cardiovascular diseases, 2014. **42**(1): p. 53-56.
22. Oyama, Y., et al., *Circadian MicroRNAs in Cardioprotection*. Current Pharmaceutical Design, 2017. **23**(25).
23. Anna, et al., *MicroRNA in cardiovascular biology and disease*. Advances in Clinical and Experimental Medicine, 2017. **26**(5).
24. Teng, S., et al., *The Role of MicroRNAs in Myocardial Infarction: From Molecular Mechanism to Clinical Application*. International Journal of Molecular Sciences, 2017. **18**(4).
25. Taylor, D.A. and A.G. Zenovich, *Cell therapy for left ventricular remodeling*. Current Heart Failure Reports, 2007. **4**(1): p. 3-10.
26. *MicroRNA-486-dependent modulation of DOCK3/PTEN/AKT signaling pathways improves muscular dystrophy-associated symptoms*. Journal of Clinical Investigation, 2014. **124**(6): p. 2651-2667.
27. Xu, J., et al., *miR-19b attenuates H2O2-induced apoptosis in rat H9C2 cardiomyocytes via targeting PTEN*. Oncotarget, 2016. **7**(10).
28. Gopal, K., et al., *FoxO1 regulates myocardial glucose oxidation rates via transcriptional control of pyruvate dehydrogenase kinase 4 expression*. Am J Physiol Heart Circ Physiol, 2017: p.

ajpheart.00191.2017.

29. Xinzheng, et al., *miR-16 controls myoblast proliferation and apoptosis through directly suppressing Bcl2 and FOXO1 activities*. *Biochimica et Biophysica Acta (BBA) - Gene Regulatory Mechanisms*, 2017.
30. *NAD(+)-dependent SIRT1 deactivation has a key role on ischemia-reperfusion-induced apoptosis*. *Vascular Pharmacology*, 2015. **70**: p. 35-44.
31. Ji, X., et al., *The Anti-fibrotic Effects and Mechanisms of MicroRNA-486-5p in Pulmonary Fibrosis*. *Rep*, 2015. **5**: p. 14131.

Figures

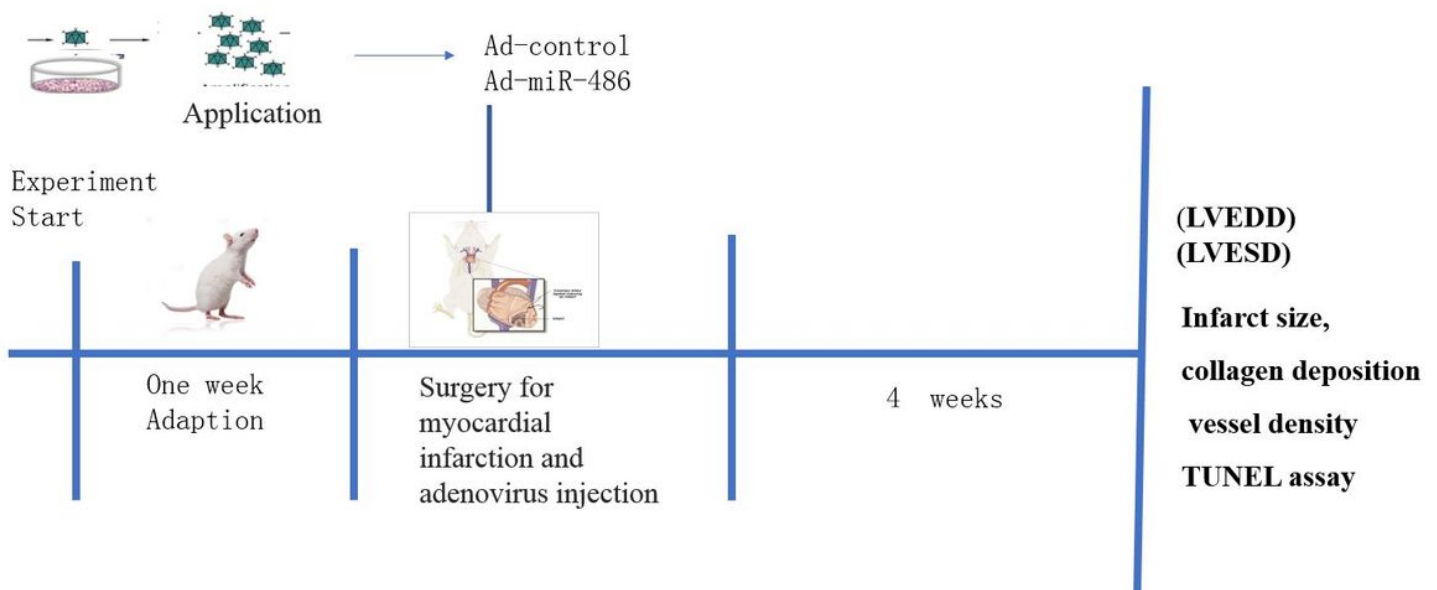


Figure 1

Workflow of the experiment. The cardiomyocytes were isolated and cultured from 1-2 day(s) old SD rats. Then, the adenovirus vector carrying rat miR-486 gene was generated and amplified to transduce cardiomyocytes with the recombinant adenovirus or miR-486 inhibitor. To establish the AMI models, the left anterior descending coronary artery was ligated in adult SD rats. The adenovirus was injected into the border zone surrounding the infarcted area. After 4 weeks, LVEDD and LVESD were measured and the rats were sacrificed for further studies.

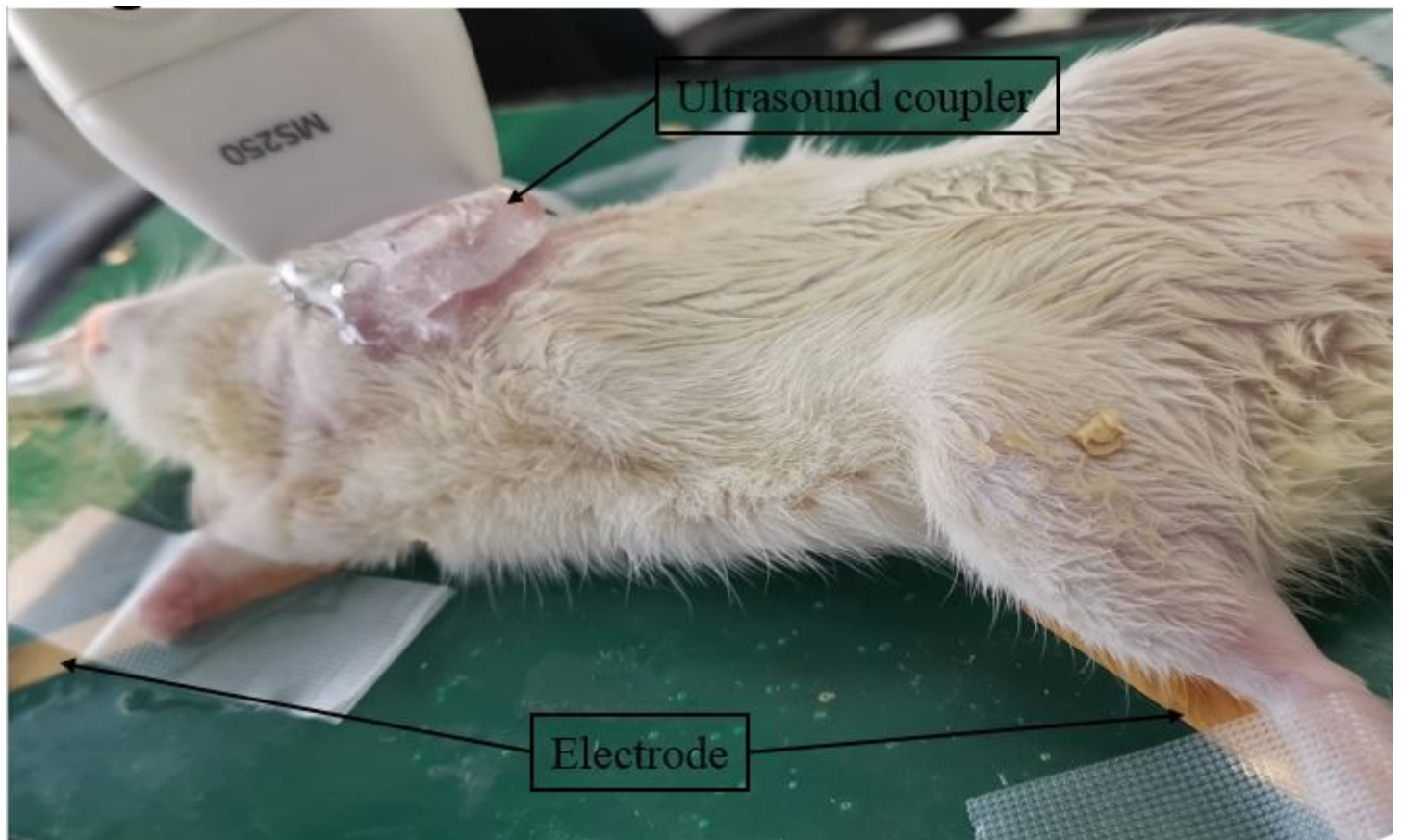


Figure 2

After anesthesia, the electrode of the Vevo770 ultrasound system was attached to the rat and the ECG was monitored. Hairs on the animal chest were removed to measure LVEDD and LVESD using an ultrasound coupler.

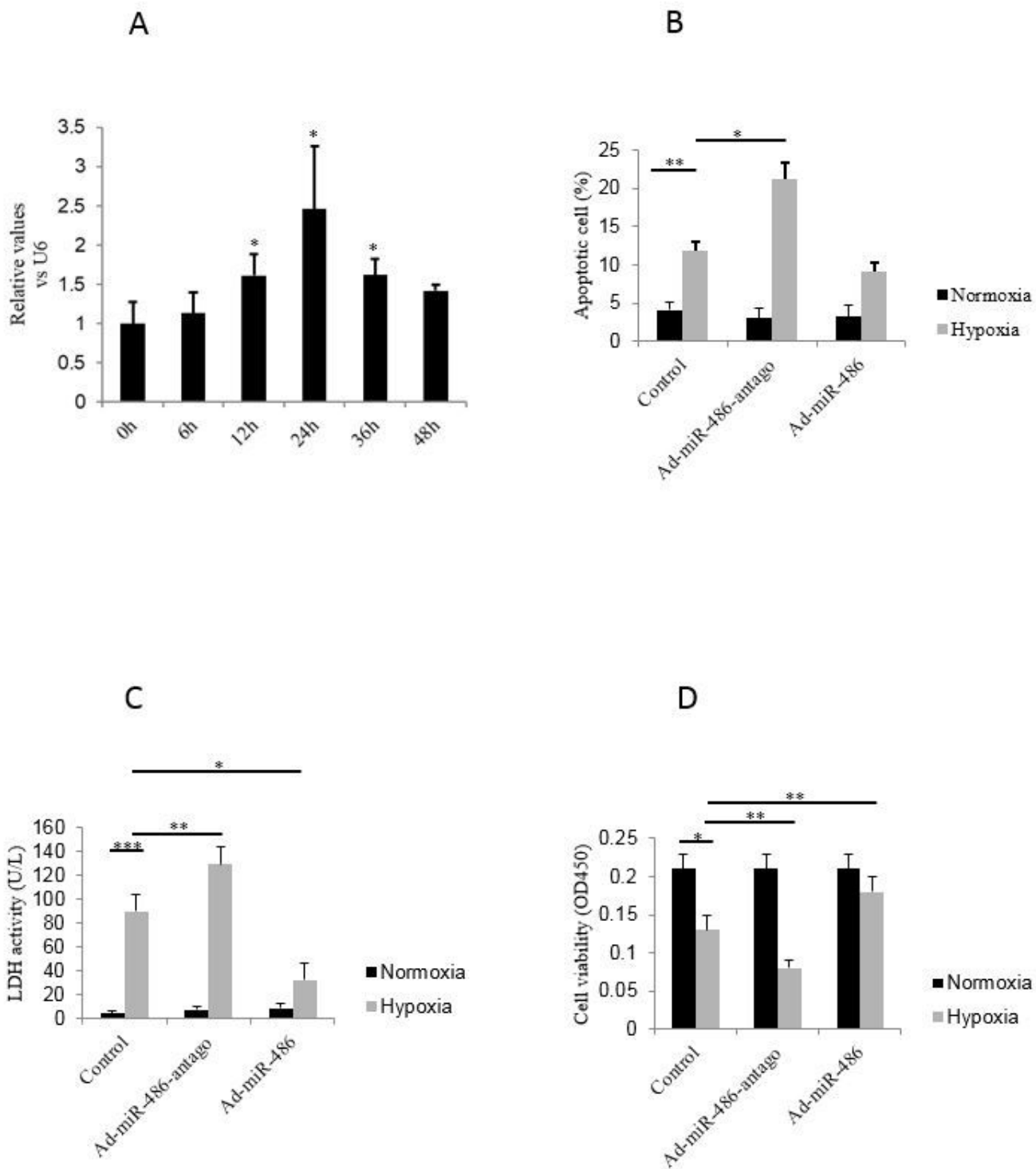


Figure 3

miR-486 expression protected cardiomyocytes from hypoxia-induced apoptosis. (A) The expression of miR-486 was determined by RT-PCR in cardiomyocytes under hypoxia. (B-D) The cardiomyocytes were transduced with miR-486 mimic or inhibitors. The cells were cultured under normoxia or hypoxia for 6 h and the (B) apoptotic index of primary cardiomyocytes, (C) LDH concentration, and (D) cell viability were determined. * $P < 0.05$, ** $P < 0.01$, *** $P < 0.001$ vs indicated group

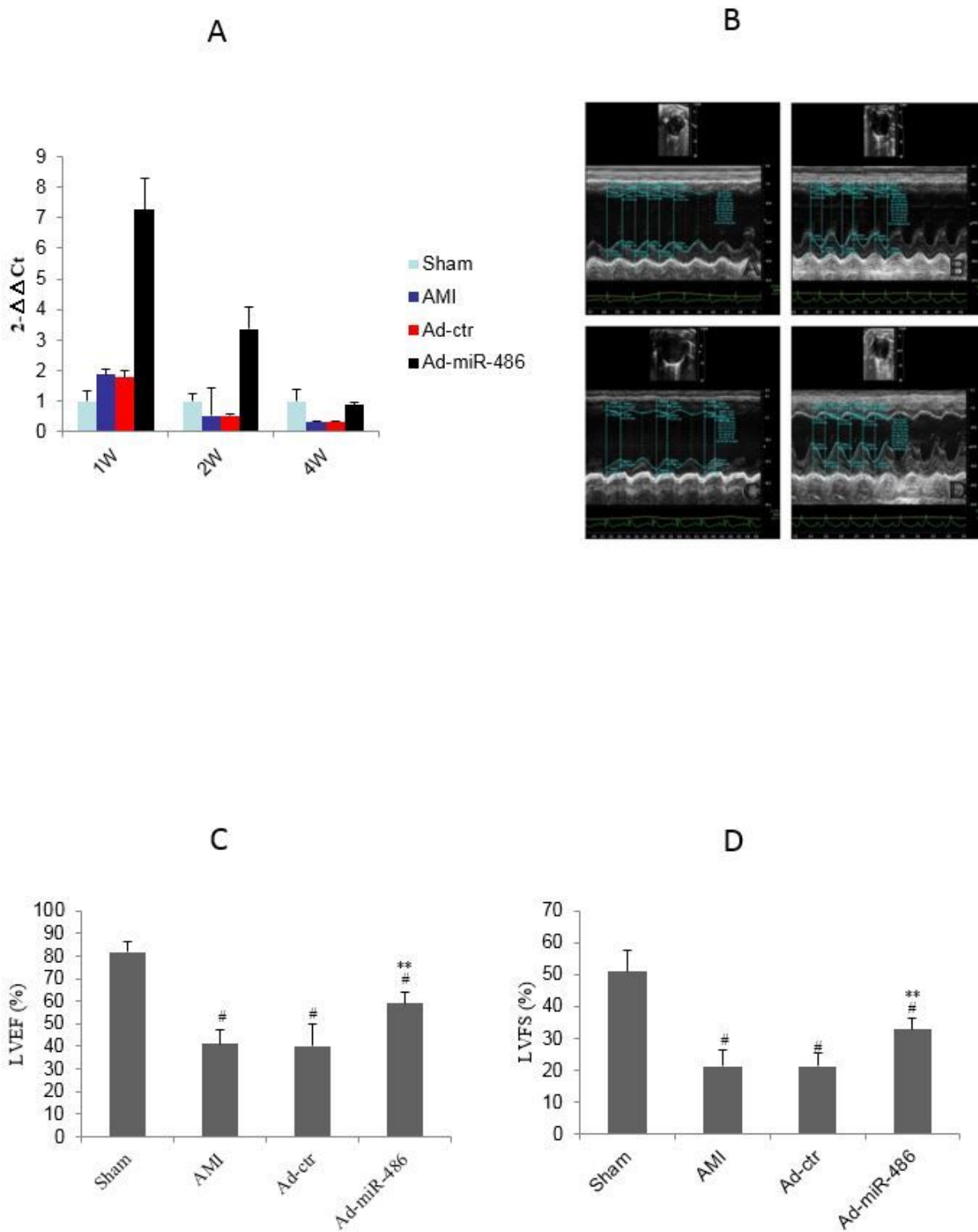


Figure 4

Adenovirus-mediated miR-486 expression improved heart function in the rat AMI model. (A) The expression of miR-486 in injected myocardium areas in the sham group, AMI group, Ad-ctr group, and miR-486 group at 1w, 2w, and 4w respectively. (B) Echocardiography of rats in the sham group, AMI group, Ad-ctr group, and Ad-miR-486 group at the end of the fourth week after AMI surgery. (C) The LVEF

and (D) LVFS of the rats in each group are shown. \square $P < 0.05$ vs Sham group; $**$ $P < 0.05$ vs AMI group and Ad-ctr group.

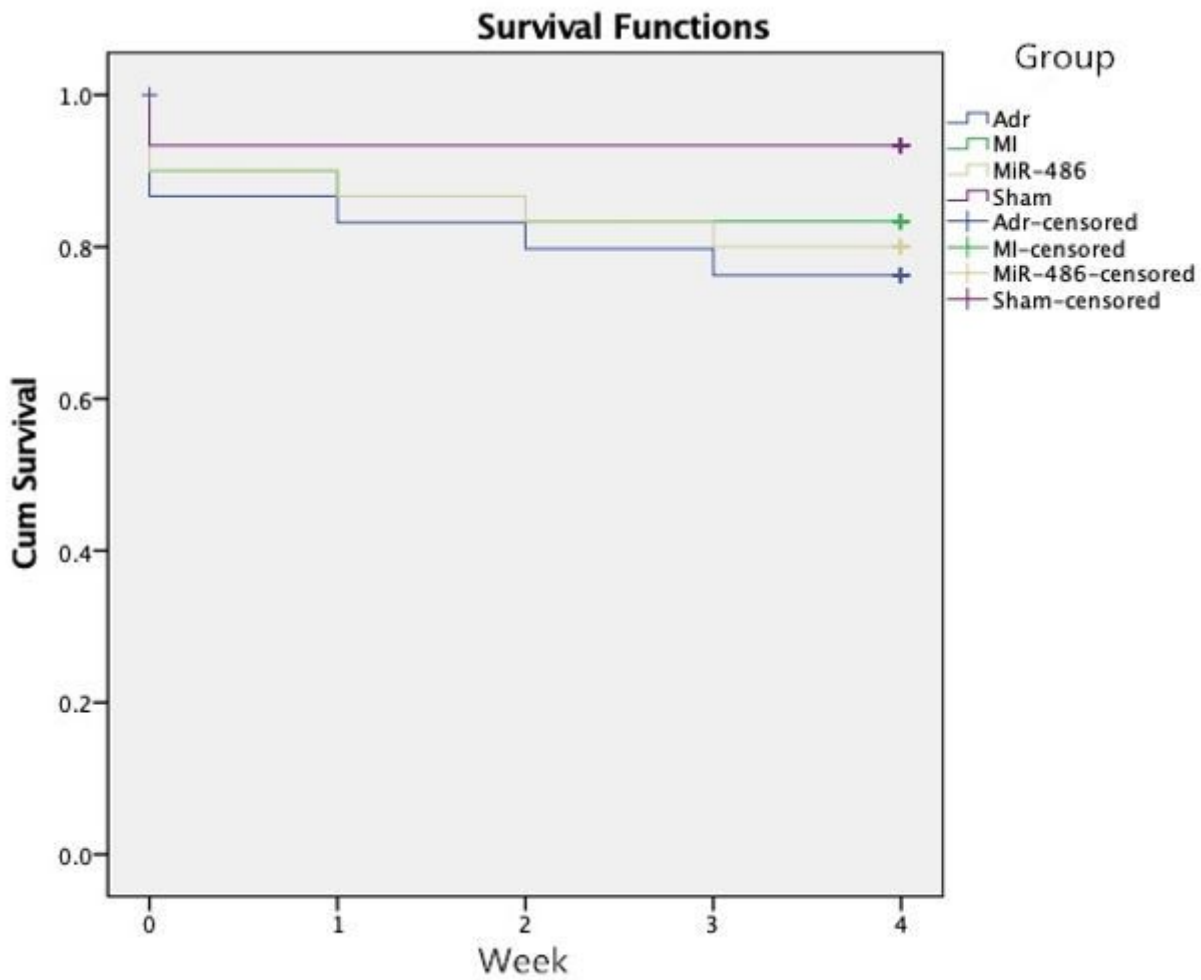


Figure 5

Survival curve of rats in all the four groups.

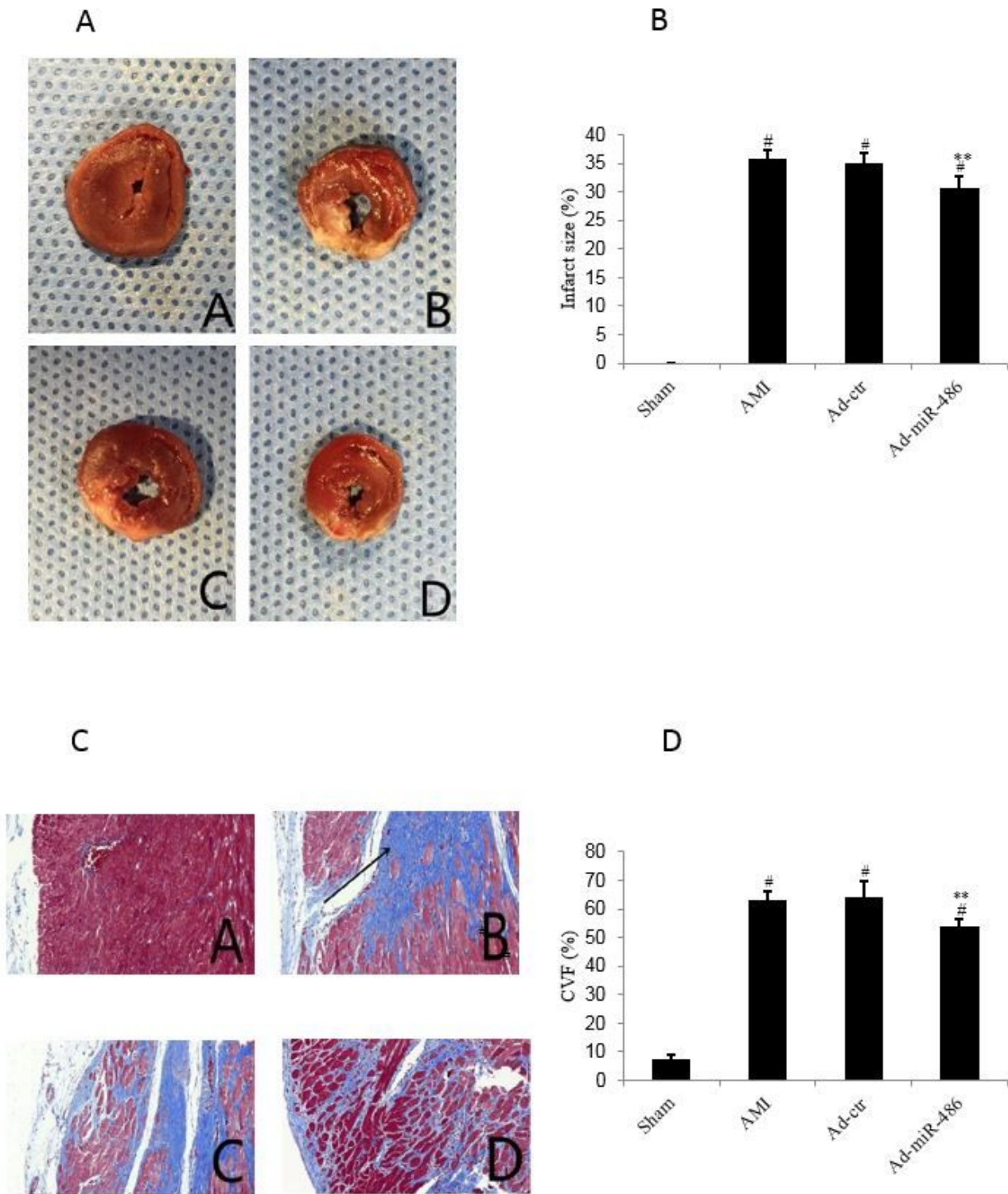


Figure 6

Ad-miR-486 transduction reduced infarct size and fibrosis in the rat AMI model. (A) Myocardial infarct size was measured by TTC staining which displayed a red color. The infarcted area is defined as TTC unstained area (white color). (B) The infarcted area data from Digital images ($\times 100$) of AMI, the different areas were pathological examined by TTC staining. (C) Digital images of collagen by Masson's trichrome staining. (D) CVF was analyzed with Image Pro-Plus 6.0 software. \boxtimes $P \leq 0.05$ vs sham group; $\boxtimes\boxtimes$ $P \leq 0.05$ vs

AMI group and Ad-ctrl group. The digital picture of A, B, C, and D is for the sham, AMI, Ad-ctrl, and Ad-miR-486 groups respectively.

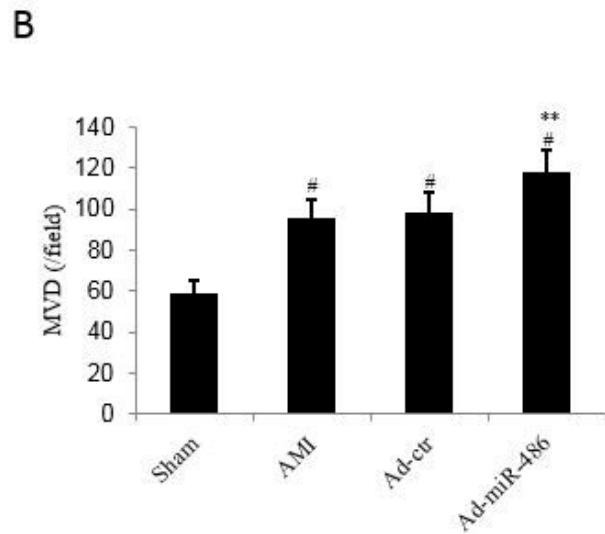
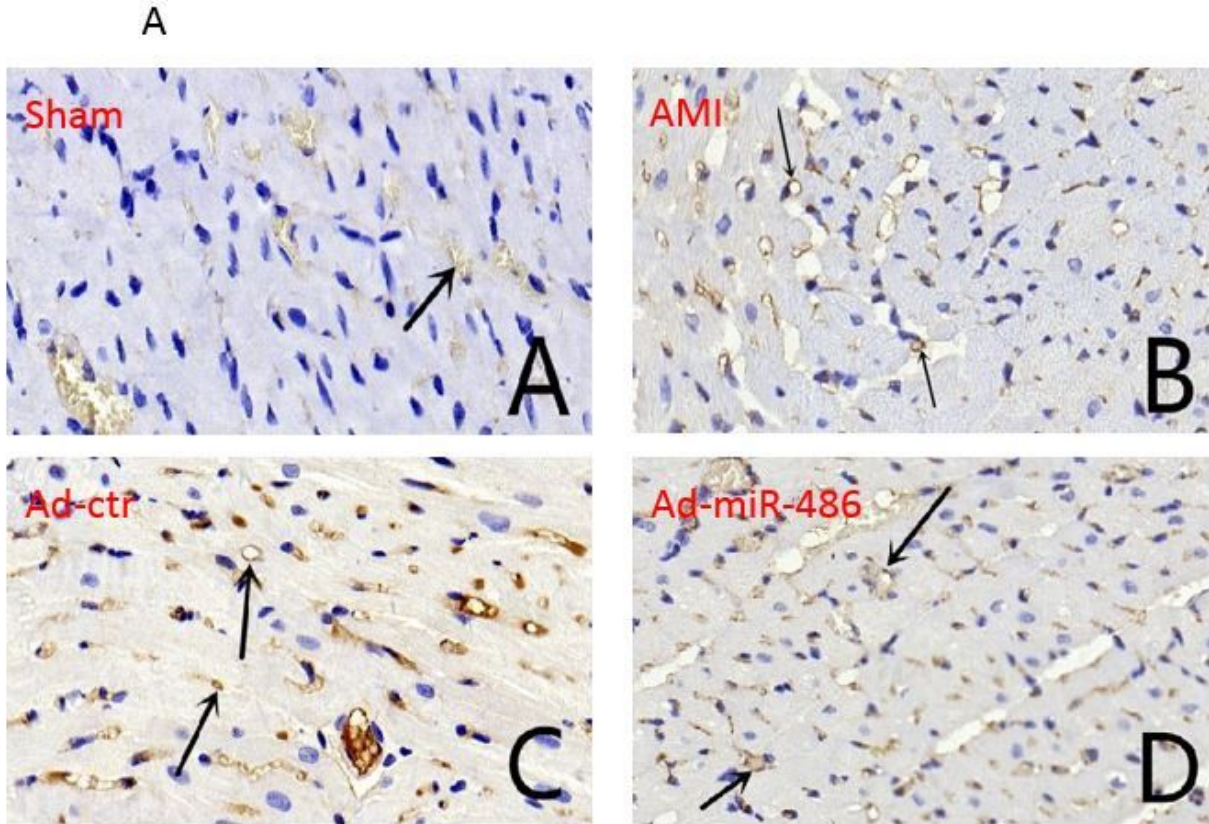


Figure 7

Ad-miR-486 transduction increased microvessel density (MVD) in the rat AMI model. (A) MVD evaluation by CD31 expression ($\times 400$); the representative views of the sham, AMI, Ad-ctrl, and Ad-miR-486 groups,

respectively at four weeks after AMI. (B) The number of MVD was calculated. \square $P < 0.05$ vs sham group; \square $P < 0.05$ vs AMI group and Ad-ctrl group.

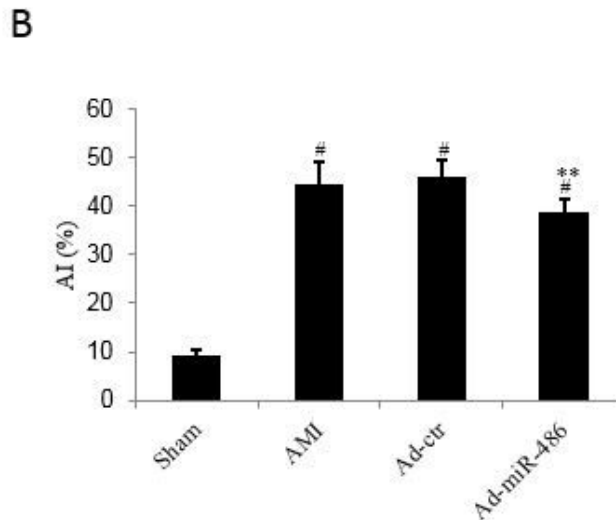
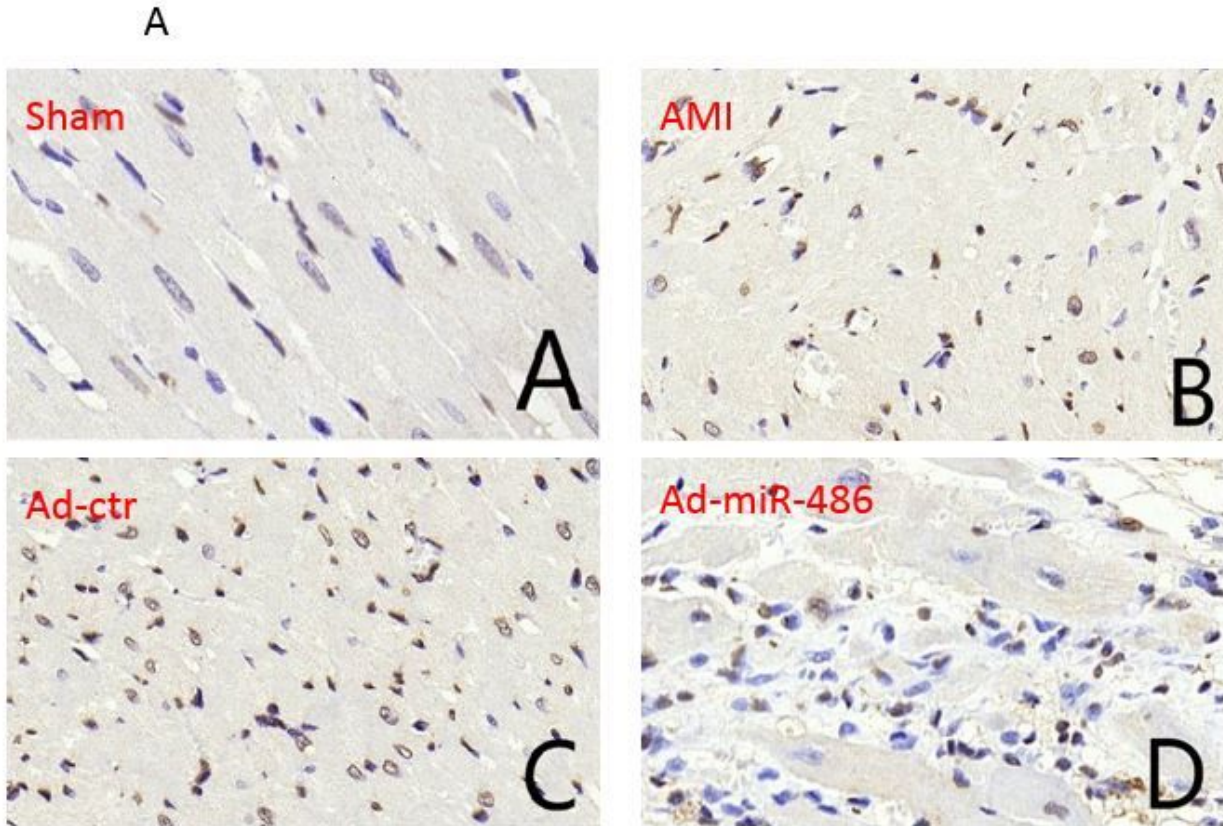


Figure 8

Ad-miR-486 transduction increased the survival of cardiomyocytes in the rat AMI model. (A) The apoptosis of cardiomyocytes was determined by TUNNEL staining. (B) Apoptosis of the cardiac cells in the infarcted areas was calculated. \square $P < 0.05$ vs sham group; \square $P < 0.05$ vs AMI group and Ad-ctrl group.